18th Brazilian Congress of Thermal Sciences and Engineering
November 16-20, 2020 (Online)

ENCIT-2020-0210
VISUALIZATION OF PULSED FLOW OF N_2O USING THE RESONANT SCHLIEREN METHOD

Danilo Almeida Machado
Fernando de Souza Costa
Associated Laboratory of Combustion and Propulsion – LABCP
Brazilian Institute for Space Research – INPE
Rodovia Presidente Dutra, km 40, CEP: 12.630-000
Cachoeira Paulista/SP – Brasil
danilo.machado@inpe.br

Dermeval Carinhana Junior
Antonio Carlos de Oliveira
Aerothermodynamics and Hypersonics Division - EAH
Institute for Advanced Studies - IEAv
Trevo Coronel Aviador José Alberto Albano do Amarante, n° 1 – Putim, CEP: 12.228-001
São José dos Campos/SP – Brasil

Abstract. *This work describes basic concepts of the resonant schlieren method and presents a discussion on the refractive index in heterogeneous media with light absorption. An experimental setup was assembled to study the pulsed flow of N_2O in ambient pressure, using a piezoelectric valve and a resonant schlieren system with a CW Nd-Yag laser in 532 nm and using iodine molecules as seeds in the flow. The results showed that the absorption of light by the iodine seeds in 532 nm makes it possible to increase significantly the contrast of the schlieren images. Therefore, the resonant schlieren method could be used in conditions where the conventional schlieren method does not present adequate contrast, such as in reactive and non-reactive flows in low pressure and in interactions between boundary layers and shock waves.*

Keywords: *optical diagnostics, flow visualization, complex refractive index, resonant schlieren.*

1. INTRODUCTION

Visualization of flows by schlieren optical methods has been one of the simplest and most used ways to qualitatively study and analyze the structure of a real flow, as well as to compare with the flow structure generated by computational methods (Settles, 2000).

Schlieren methods are again in the state of the art in the field of optical flow diagnostics and now can be used to determine quantitatively the velocity, temperature and density fields within the flows. Modern schlieren methods include SIV (schlieren image velocimetry) to determine flow velocities (Hargatherv, et al. 2011). Rainbow Schlieren to determine densities and temperatures (Feikema, 2006). BOS (background oriented schlieren) ability to measure image large and three-dimensional fields of velocity, density and temperature (Nicolas, et al. 2016). Resonant Schlieren that uses absorption of light by the molecules or atoms in the flow to increase the sensitivity of the technique, for applications where the conventional schlieren method has too low contrast (Merzkirch, 2012).

The sensitivity of schlieren methods depends on the variation of the refractive index of the medium and the characteristics of the optical instruments used in the arrangement. Light is transmitted uniformly through homogeneous means in a straight line. On the other hand, when light crosses heterogeneous media it is deflected due to the non-uniformity of the refractive index.

Transient regimes such as subsonic to supersonic are accompanied by instabilities and shock waves. These phenomena are a challenge to be predicted by computational models and characterized by experiments. The design of aerospace propulsion systems requires the use of highly accurate theoretical models of aerothermodynamics. The success of a project depends on the design ability to accurately predict the behavior of each component.

In the development of aerospace vehicles, commercial or in-house fluid dynamics software is normally used, nevertheless there is a need to validate the theoretical results with experimental data. Experimental measurements of parameters such as temperature, velocity and density can be used to adjust theoretical models.

Lemieux and Hornung (2002) used the Resonant schlieren technique to investigate Tollmien-Schlichting instabilities and flow regime transitions. Interactions of the shock layer with the boundary layer in high enthalpy hypersonic flows

were observed. Bishop et. al. (2004) improved the resonant schlieren method for determining the density in acetylene flames without the need for prior combustion information such as temperature and pressure.

This work presents the fundamentals of the resonant schlieren method and derives the Kramers-Kronig relations to determine the complex refractive index. The spectrum of I_2 was simulated using the code IodineSpec5 to determine the absorption wavelengths of I_2. Images of pulsed flows of N_2O with sublimated I_2 seeds were obtained using resonant schlieren method at ambient pressure, and the contrasts of resonant schlieren images were compared to conventional schlieren images.

2. METODOLOGY

The methodology section is divided in three sections. The first section presents the schlieren method, fundamentals of the angular deflection of light, and the contrast of the schlieren image. The second part describes the complex refractive index, and the relationship between atomic and molecular absorption and refractive index. The third part presents the experimental setup.

2.1 Schlieren theory

A detailed description of the schlieren methods is given by Machado et al. (2020). Figure 1 shows a typical schlieren optical arrangement, using a light source, one lens to collimate the light beam, another lens to focus the light beam, an optical filter, known as “knife”, and a screen where the flow image is formed.

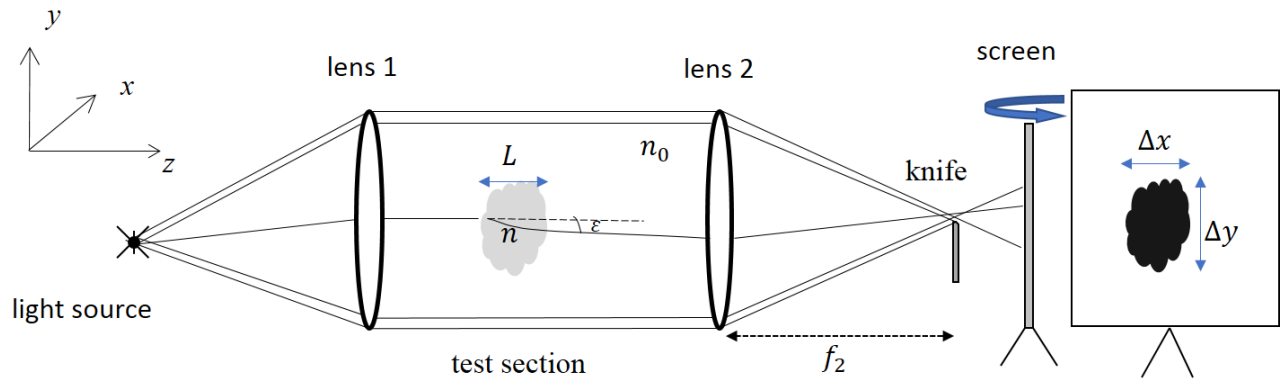

Figure 1. Schlieren system with light source, two lenses, an optical filter (knife) and a screen.

The basic principle of the schlieren technique is the deflection of light passing through a heterogeneous medium. As shown in Fig. 1, the light rays passing through the test object between lenses 1 and 2, undergo refraction due to the density gradient of the object, since the refractive index is directly proportional to density. The refractive index is given by $n = 1 + k_{GD}\rho$, where k_{GD} is the Gladstone-Dale constant.

A fraction of the rays passing through the test object is blocked by the knife, increasing the contrast of the image on the screen. The deflection in the y direction of a beam of light that passes in the z direction through a heterogeneous medium is given by:

$$\varepsilon_y = \frac{L}{n_0}\frac{\partial n}{\partial y} \tag{1}$$

where n_0 is the refractive index of the surrounding medium, n is the refractive index of the object and L is the length in the z direction of the object.

The contrast C is the variation ratio of the ΔE illuminance to the background illuminance E, in a schlieren image, given by $C \equiv \Delta E/E = (f_2\varepsilon_y/a)$, where f_2 is the focal distance of the second lens (see Fig.1) and a is the unobstructed height of the source image formed on the knife. The contrast of a schlieren image is given by:

$$C = \frac{f_2}{a}\frac{L}{n_0}\frac{\partial n}{\partial y} = \frac{f_2}{a}\frac{Lk}{1 + k\rho_0}\frac{\partial \rho}{\partial y} \tag{2}$$

2.2 Complex refractive index

To describe the refractive index with absorption, the classic model of a forced damped oscillator can be used, based on Maxwell's equations of electrodynamics. The result is a complex refractive index obtained from Kramers-Kronig relations. Details of the following theoretical background are presented by Demtröder (1996) and Hecht (2002).

The intensity of light when passing through an absorbent medium is given by Beer's Law:

$$I = I_0 e^{-\alpha(\omega)z} \tag{3}$$

where Io is the intensity of the incident light, I is the intensity of the light at a distance z within the medium, $\alpha(\omega)$ is the absorption coefficient and ω is the angular frequency of the light.

The absorption profile $\alpha(\omega)$ can be obtained from the classic model of an oscillator damped with load q under the influence of a force qE caused by an incident wave, with the amplitude of the electric field E given by:

$$E = E_0 e^{i\omega t} \tag{4}$$

The intensity of the electric field can be written in the form of the differential equation:

$$m\ddot{x} + \dot{m}x + kx = qE_0 e^{i\omega t} \tag{5}$$

where m is the mass of the absorbing element. After solving this differential equation, the induced magnetic dipole moment $p = qx$ can be determined by the forced oscillation of a charge q. Considering N oscillators per volume unit, with a polarization P, which is the sum of all dipole moments per volume unit, given by:

$$P = Nqx = \frac{Nq^2E}{m(\omega_0^2 - \omega^2 + i\gamma\omega)} \tag{6}$$

Polarization can also be obtained in a different way, from Maxwell's equations of classical electrodynamics:

$$P = \epsilon_0(\epsilon - 1)E = \epsilon_0\chi E \tag{7}$$

where ϵ_0 is the dielectric constant and χ is the electrical susceptibility of the dielectric.

From Maxwell's equations, the velocity of an electromagnetic wave in a medium with dielectric constant $\epsilon_0\epsilon$ and with magnetic permeability $\mu_0\mu$ is given by:

$$v = (\epsilon_0\epsilon\mu_0\mu)^{-1/2} \tag{8}$$

Knowing that the refractive index is defined as $n = c/v$ where $c = (\epsilon_0\mu_0)^{-1/2}$ is the velocity of light in a vacuum, then $n = \sqrt{\epsilon\mu}$. Considering μ≅1, except in ferromagnetic media, then $n = \sqrt{\epsilon}$.

Combining Eqs. 6 and 7 and using $n = \sqrt{\epsilon}$, results:

$$n^2 = 1 + \frac{Nq^2}{m\epsilon_0(\omega_0^2 - \omega^2 + i\gamma\omega)} \tag{9}$$

Gases at low pressure have $n \cong 1$, then $n^2 - 1 \cong 2(n-1)$, therefore:

$$n = 1 + \frac{Nq^2(\omega_0^2 - \omega^2 + i\gamma\omega)}{2m\epsilon_0(\omega_0^2 - \omega^2 + i\gamma\omega)} \tag{10}$$

For example, atmospheric air has a refractive index of 1.00028 for the wavelength of 500 nanometers. Separating the real part of the result from its imaginary part, one can rewrite Eq. (10) as:

$$n = n' - i\kappa \tag{11}$$

where n is the complex refractive index, n' is the refractive index and κ is the attenuation coefficient for absorption.

The electric field equation of an electromagnetic wave propagating in the z direction is $E = E_0 e^{i(\omega t - kz)}$ in a medium with a refractive index n, with a frequency ω_n equal to the frequency ω_0 in a vacuum. However, the wave number is given by $k_n = k_0 n$, where $|k| = 2\pi/\lambda$, where λ is the wavelength. Inserting $n = n' - i\kappa$, the electric field equation is:

$$E = E_0[e^{-k_0\kappa z}]\left[e^{i(\omega t - k_0 n' z)}\right] = E_0\left[e^{-2\pi\kappa z/\lambda_0}\right]\left[e^{ik_0(ct - n' z)}\right] \tag{12}$$

The Eq. 12 shows that the imaginary part $\kappa\ (\omega)$ of the complex refractive index n describes the absorption of an electromagnetic wave. With a penetration depth $\Delta z = \lambda_0/(2\pi\kappa)$, the amplitude of the electric field decreases from $E_0 e^{-k_0 kz}$ to 1 / and 1/e from its value at $z = 0$. The real part $n'(\omega)$ represents the dispersion of the wave, that is, the dependence of the phase velocity $v(\omega) = c/n'(\omega)$ with the frequency. Intensity I is proportional to EE^* and decreases as:

$$I = I_0 e^{-2\kappa k_0 z} \tag{13}$$

Eq. 13 is related to Beer's law, it can be deduced that the absorption coefficient can be written as:

$$\alpha = 2\kappa k_0 = \frac{4\pi\kappa}{\lambda_0} \tag{14}$$

Therefore, the absorption coefficient is proportional to the imaginary part κ of the complex refractive index. Combining Eqs. 14, 11 and 10 and separating the real and imaginary parts:

$$\alpha = \frac{Nq^2\omega_0}{c\epsilon_0 m}\frac{\gamma\omega}{(\omega_0^2 - \omega^2)^2 + \gamma^2\omega^2} \tag{15a}$$

$$n' = 1 + \frac{Nq^2}{2\epsilon_0 m}\frac{\omega_0^2 - \omega^2}{(\omega_0^2 - \omega^2)^2 + \gamma^2\omega^2} \tag{15b}$$

These are the Kramers-Kronig dispersion relations where absorption and dispersion are related through the complex refractive index, rewritten as:

$$n = n' - i\kappa = n' - \frac{i\alpha}{2k_0} \tag{16}$$

Therefore, an increase in the absorption coefficient implies a higher value for the complex refractive index module. In the case of molecular absorption transitions, the transition frequency $\omega_0 \gg |\omega_0 - \omega|$ with $q = e$, it results:

$$\alpha(\omega) = \frac{Ne^2}{4c\epsilon_0 m}\frac{\gamma}{(\omega_0^2 - \omega^2)^2 + (\gamma/2)^2} \tag{17a}$$

$$n' = 1 + \frac{Ne^2}{4\epsilon_0 m\omega_0}\frac{\omega_0 - \omega}{(\omega_0^2 - \omega^2)^2 + (\gamma/2)^2} \tag{17b}$$

The molecular absorption profile $\alpha(\omega)$ is a Lorentzian, with a width at half height of $\Delta\omega_n = \gamma$, which is equal to the width at half natural height.

2.3 Resonant Schlieren

The principle of resonant schlieren is to seed atoms or molecules in a flow, so that these particles absorb in the wavelength of the light source, causing an increase in the contrast of the flow image. Figure 2 shows the image of the normal schlieren in (*a*) and the resonant schlieren in (*b*).

Figure 2 (*a*) shows the normal schlieren system, where the flow was not seeded by absorbent particles. The normal lines represent the rays of light that have not changed in their path, the dashed lines with two points represent the rays of light that have been deflected. In (*b*) we have the resonant schlieren system, the dashed lines correspond to the rays of light that are absorbed.

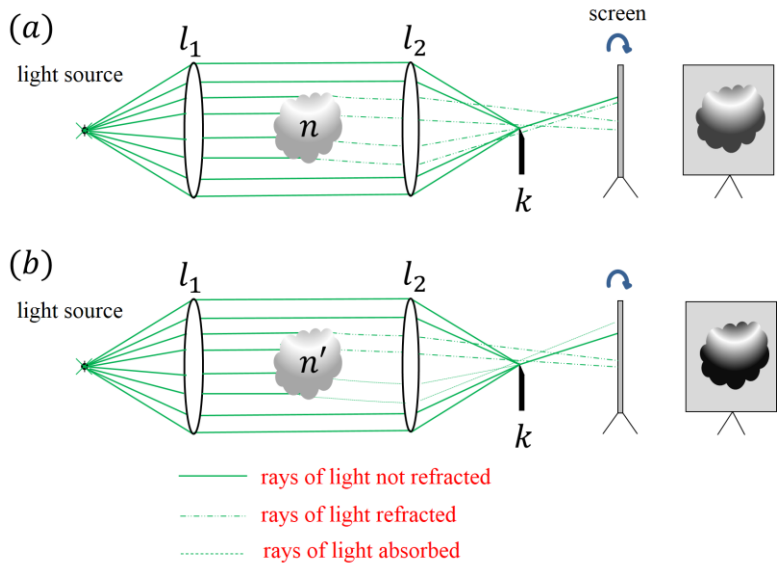

Figure 2. Schema of schlieren systems, where l_1 is the first lens, l_2 is the focusing lens and k is the knife. The medium with refractive index n corresponds to the pure flow and n' corresponds to the flow with absorbent seeds. In (a) is the conventional schlieren system, in (b) is the resonant schlieren system.

2.4 Experimental Methodology

Figure 3 shows the experimental setup. It includes the schlieren system, a stainless-steel expansion chamber, a pulsed piezoelectric valve model 203B LPV, an oscilloscope model Tektronix TDS 2014, a function generator model FG-2002C, a N_2O tank with pressure 500 kPa, an iodine cell, and a valve driver to amplify the signal from the function generator to open the valve. The pressure was measured by Pirani's portable thermovac model TM 101.

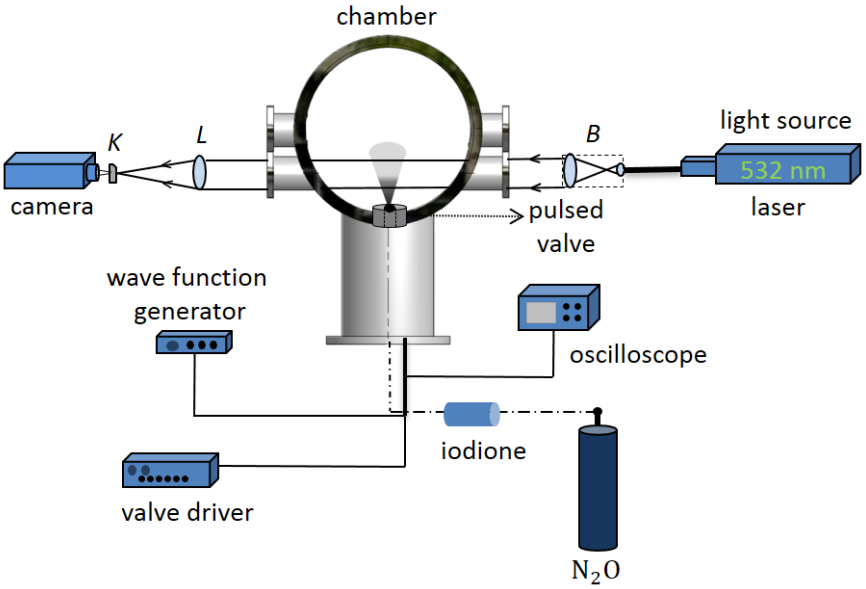

Figure 3. Experimental arrangement of the resonant schlieren, where B is the laser beam expander, L is the focusing lens and K is the knife.

The experimental method consists of analyzing the resonant schlieren images using a laser as a light source, with emission at 532 nm. In the 532 nm wavelength region, there are absorption lines for the iodine molecule. Absorption in this region causes an increase in the refractive index of the medium, which was demonstrated in the complex refractive index equation.

To compare results, measurements were made at this wavelength without the addition of iodine seeding. To seed the iodine in the flow, a premix capsule with a thermal jacket was added to facilitate the sublimation of the iodine. The flow of N_2O as it passes through the capsule encounters the iodine molecules, which are expanded together by the pulsed valve in the chamber.

3. RESULTS AND DISCUSSIONS

By equating the complex refractive index, an increase in its value is expected due to the absorption of light by the iodine seeds, this effect causes an increase in the contrast in the schlieren image, since the schlieren effect is proportional to $\partial\rho/\partial y$. Figure 4 shows an image of the experimental system that was assembled at the Molecular Spectroscopy Laboratory of the Institute for Advanced Studies at DCTA. In Figure 3 the items with numbers are: (1) laser; (2) prisms; (3) beam expander; (4) expansion chamber; (5) focusing lens; (6) optical filter (knife); (7) high speed camera; (8) driver, wave function generator and oscilloscope.

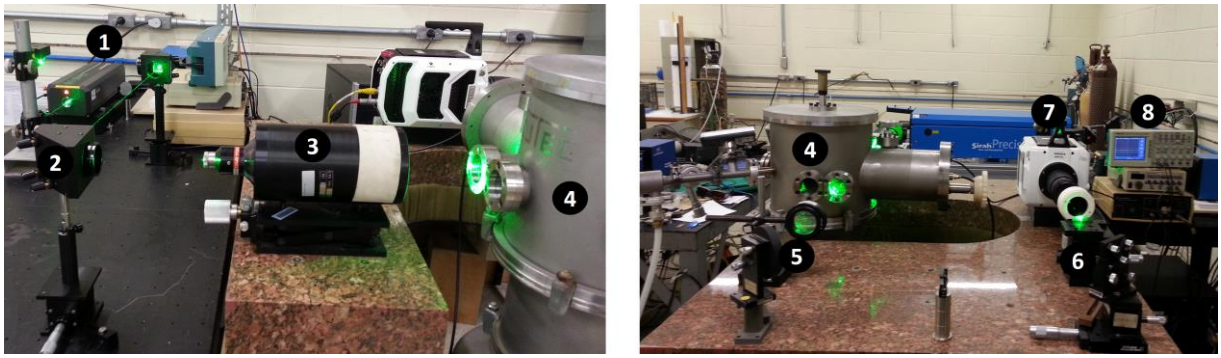

Figure 4. Pictures of the experimental arrangement of the resonant schlieren.

Figure 5 shows a simulation of the absorption spectrum of iodine molecules, obtained with the IodineSpec5 code. Intensity values are normalized with maximum value assumed as 1.0. The region of the wavelength from 514.5259 to 721.2673 nm was simulated, with 13239 different wavelengths. The refractive index of air was considered $n = 1.000277$, with temperature 293.0 K and line width of $0.005\ cm^{-1}$. As seen in Fig. 5 there are strong absorption lines in the 532.0 nm region.

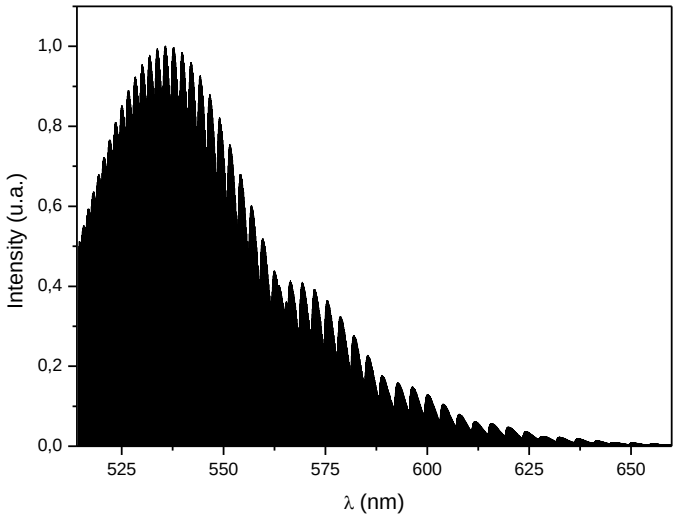

Figure 5. Iodine absorption spectrum.

The iodine absorption spectrum appears continuous, similar to a blackbody spectrum. However, when investigating a small wavelength range, it is noted that absorption is discretized. Figure 6 shows the same absorption spectrum in the region from 531.5 to 532.5 nm, and the discretized absorption lines can be noted. The iodine molecule was chosen to be seeded in the flow, because it has absorption lines in the region of 532.0 nm, a common wavelength for lasers with continuous wave.

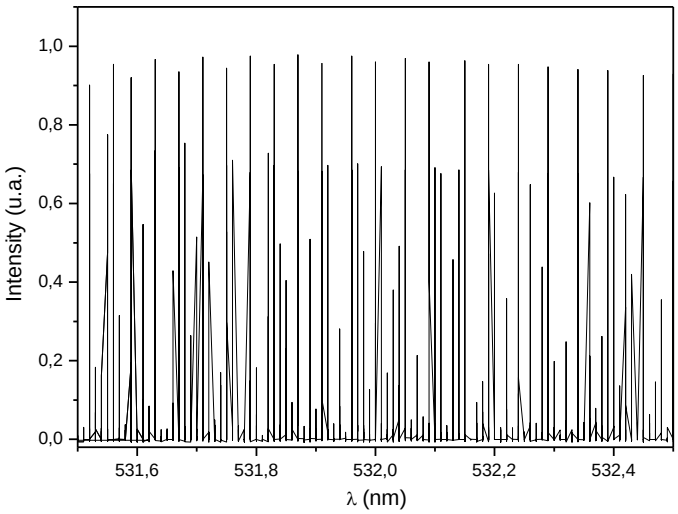

Figure 6. Iodine spectrum, with absorption lines.

Figure 7 shows schlieren images obtained from the flow of N_2O from a pulsed valve. Figure 7 (*a*) shows the image of the test section without the flow, Figure 7 (*b*) shows the image of pure N_2O flow and Figure 7 (*c*) the flow of N_2O with seeds of iodine. As seen in Fig. 7 the presence of iodine in the flow increases the contrast in the schlieren image. Artifacts in the image come from diffraction of the laser coherent light through the lenses.

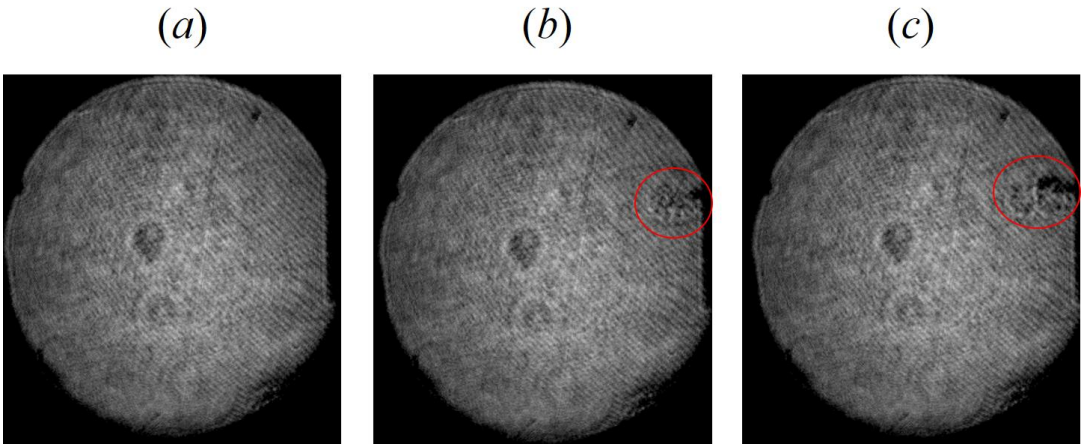

Figure 7. Schlieren images of a flow of N_2O. In (*a*) is the image of the test area without the flow; (*b*) image of the flow of pure N_2O; (*c*) image of the flow with iodine seeds.

The results indicate that iodine seeds can be used in situations where the conventional schlieren is unable to produce images, for example, flows produced at low pressure. In addition, the resonant schlieren with iodine seeds can be used in shock tunnels, to observe effects such as interaction of the shock layer with the limit layer in different Mach Numbers.

4. CONCLUSIONS

The work described the resonant schlieren method and derived the complex refractive index equations. The spectrum of I_2 was simulated to determine its absorption wavelengths. An experimental setup for studying the pulsed flow of N_2O was prepared to apply the resonant schlieren method using a CW Nd-Yag laser in 532 nm, using iodine molecules as seeds in the flow. The results obtained have showed that the absorption of light by the iodine seeds makes it possible to increase significantly the contrast of the schlieren technique in ambient pressure. Consequently, the resonant schlieren method could be used in conditions where the conventional schlieren method has low contrast, such as in reactive and non-reactive flows at low pressure conditions.

5. ACKNOWLEDGEMENTS

CAPES for the granting of the PHD scholarship and FINEP for the financing of the CSLASER project.

6. REFERENCES

Bishop, A.I., McIntyre T. J., Littleton B. N. e Rubinsztein-Dunlop H., 2004. "Near-resonant holographic interferometry and absorption measurements of seeded atomic species in a flame". *Applied Optics*, Vol. 43, No. 17, pp. 3391-3400.

Demtröder, W., 1996. *Laser Spectroscopy - Basic Concepts and Instrumentation*, Springer-Verlag Berlin Heidelberg, New York, 2nd edition.

Feikema, D.A., 2006. "Quantitative rainbow schlieren deflectometry as a temperature diagnostic for nonsooting spherical flames", *Applied Optics*. Vol. 45, No. 20, pp. 4826-4832.

Germain, P. e Hornung, H., 1997. "Transition on a slender cone in hypervelocity flow". *Experiments in Fluids*, Vol. 22, pp. 183–190.

Hargather, M.J., Lawson, M.J., Settles, G. S. and Weinstein, L. M., 2011. "Seedless velocimetry measurements by Schlieren Image Velocimetry". *AIAA Journal*, Vol. 49, No. 3, pp. 611–620.

Hecht, E., 2002. *Óptica*. Fundação Calouste Gulbenkian, Lisboa, 2nd edition.

Lemieux, P. e Hornung, H., 2002. "Development and application of streak line visualization in hypervelocity flows". *Experimets in Fluids*, Vol. 33, pp. 188–195.

Machado, D. A., Costa, F. S., Carinhana, D. J., Oliveira, A. C., 2020. "Visualização de Escoamentos pelos Métodos Ópticos Shadowgraph e Schlieren". *Revista Brasileira de Ensino de Física*. Vol. 42.

Merzkirch W., 2012. *Flow Visualization*, Academic Press, 2nd edition

Nicolas, F. et al. 2016. "A direct approach for instantaneous 3D density field reconstruction from background-oriented schlieren (BOS) measurements". *Expiments in Fluids*, Vol. 57, No. 13.

Knöckel H. and Tiemann E., 2011, "Program IodineSpec5". 20 July 2020, < https://www.iqo.uni-hannover.de/ >

7. RESPONSIBILITY NOTICE

The authors are the only responsible for the printed material included in this paper.